Role of atmospheric adjustments in the tropical Indian Ocean warming during the 20th century in climate models

Yan Du[1,2] and Shang-Ping Xie[1,3]

Received 13 February 2008; accepted 21 March 2008; published 23 April 2008.

[1] The tropical Indian Ocean has been warming steadily since 1950s, a trend simulated by a large ensemble of climate models. In models, changes in net surface heat flux are small and the warming is trapped in the top 125 m depth. Analysis of the model output suggests the following quasi-equilibrium adjustments among various surface heat flux components. The warming is triggered by the greenhouse gas-induced increase in downward longwave radiation, amplified by the water vapor feedback and atmospheric adjustments such as weakened winds that act to suppress turbulent heat flux from the ocean. The sea surface temperature dependency of evaporation is the major damping mechanism. The simulated changes in surface solar radiation vary considerably among models and are highly correlated with inter-model variability in SST trend, illustrating the need to reduce uncertainties in cloud simulation. **Citation:** Du, Y., and S.-P. Xie (2008), Role of atmospheric adjustments in the tropical Indian Ocean warming during the 20th century in climate models, *Geophys. Res. Lett.*, *35*, L08712, doi:10.1029/2008GL033631.

1. Introduction

[2] The tropical Indian Ocean (TIO) has displayed a steady increase in sea surface temperature (SST) since the 1950s, with the trend in basin-mean SST amounting to 0.5°C by the end of 20th century. Figure 1a shows the observed trend normalized by the standard deviation of detrended SST variability. By this signal-to-noise ratio measure, the TIO stands out as the region with the most robust warming for the past six decades. Atmospheric general circulation model (GCM) studies suggest that the TIO warming induces changes in African Sahel rainfall [*Giannini et al.*, 2003] and the North Atlantic Oscillation [*Hoerling et al.*, 2004], and influences the extratropical teleconnections of El Niño/the Southern Oscillation (ENSO) [*Lau et al.*, 2006]. Evidence for climatic influence of TIO warming is also emerging on interannual timescales, especially during the summer following El Niño [*Yang et al.*, 2007].

[3] Coupled ocean-atmosphere GCMs forced with increased greenhouse gas (GHG) concentrations simulate a warming trend over the TIO [*Pierce et al.*, 2006; *Knutson et al.*, 2006; *Alory et al.*, 2007]. Figure 1b shows the time series of TIO SST simulated by 11 coupled GCMs participating in the Intergovernmental Panel on Climate Change Fourth Assessment Report (IPCC AR4), in the Climate of the 20th Century runs forced with observed history of GHG concentrations, solar radiation, and other climate forcing. All the models capture the TIO warming, with variability in the onset and magnitude of the trend. Determining the cause of TIO warming in observations proves difficult; *Yu et al.* [2007] report that the 1988–2000 trend in net surface heat flux (NHF) is very small over the TIO compared to differences among products examined. In models, specific mechanisms for the TIO response to the GHG forcing remain unclear. In fact, as we will show, the TIO-mean NHF trend is virtually zero, leading to a puzzle of how the TIO warms up in the first place with very weak net surface heating.

[4] The present study investigates ocean-atmospheric adjustments to increased GHG forcing by examining changes in various components of surface heat flux. Our initial hypothesis is that in response to the increased GHG forcing, TIO climate adjusts, say by increasing SST and latent heat flux (LHF), to offset this downward heat flux so that the net flux remains unchanged. This quasi-equilibrium warming is possible because of the slow timescale. The ocean heat storage due to the 0.5°C warming in a 150 m layer over 50 years requires a NHF less than 0.2 W/m^2, much smaller than the GHG-induced increase in downward longwave radiation (DLR) estimated at about 1 W/m^2 for the same period. This quasi-equilibrium adjustment has important implications for detecting the cause of TIO warming from surface heat flux observations; instead of NHF, one should examine larger component fluxes. While radiative balance is routinely analyzed at the top of the atmosphere to study climate feedback [*Bony et al.*, 2006], to our knowledge, a similar heat flux analysis has not been performed at the TIO surface where turbulent flux is important. By studying how component fluxes reach quasi-equilibrium, we aim to identify atmospheric adjustments important for the ocean response to global warming.

2. Data

[5] The World Climate Research Program's (WCRP) Third Coupled Model Intercomparison (CMIP3) multi-model dataset is obtained from https://esg.llnl.gov:8443/index.jsp. The abbreviated model names follow the *Intergovernmental Panel on Climate Change* (*IPCC*) [2007, Table 8.1] convention. We choose 11 models for analysis based on their simulations of Indian Ocean climate including its seasonal cycle. Similar results are obtained with a larger model ensemble. The analysis period is from January 1900 to December 1999. Surface variables from models, such as heat flux, SST, wind, and humidity, are from all the ensemble runs available while subsurface ocean temperature

[1]International Pacific Research Center, SOEST, University of Hawaii at Manoa, Honolulu, Hawaii, USA.
[2]Key Laboratory of Tropical Marine Environmental Dynamics, South China Sea Institute of Oceanology, Chinese Academy of Sciences, Guangzhou, China.
[3]Department of Meteorology, SOEST, University of Hawaii at Manoa, Honolulu, Hawaii, USA.

0094-8276/08/2008GL033631$05.00

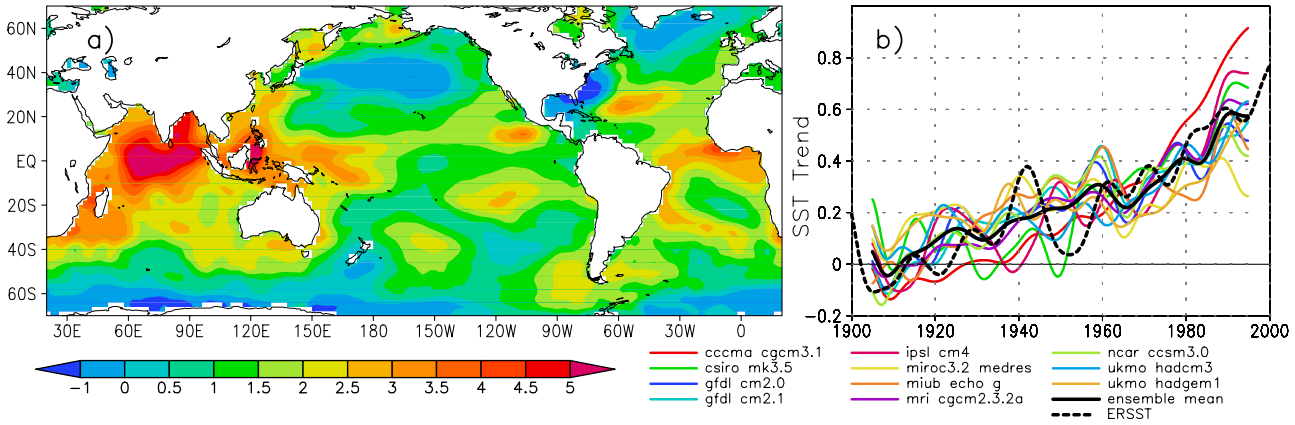

Figure 1. Observed and simulated SST trend. (a) Ratio of the trend to the standard deviation of the detrended yearly SST in ERSST observations for 1947 December–2007 November. (b) SST deviation (°C) from the 1900-04 mean in ERSST and 11 coupled models, averaged over the TIO basin (40°–120°E, 20°S–20°N). For each model, the ensemble mean of the CMIP3 20th century runs is shown. A 10-year low-pass filter has been applied.

is from only one ensemble member of each model except the MIUB model, which has no subsurface temperature available. We use the extended reconstructed SST (ERSST) [*Smith and Reynolds*, 2004] for observations.

3. Surface Heat Flux Adjustment

[6] Surface heat flux consists of four components: solar radiation, net DLR, sensible and latent heat fluxes. Latent heat flux (LHF), in particular, may be cast as

$$Q_E = \rho_a L C_E W [q_s(T) - RH \cdot q_s(T - \Delta T)], \qquad (1)$$

where ρ_a is surface air density, L the latent heat of evaporation, C_E the transfer coefficient, W surface wind speed, $q_s(T)$ is the saturated specific humidity following the Clausius–Clapeyron equation, RH surface relative humidity, T is SST, and ΔT the sea minus air surface temperature difference. Changes in both atmospheric conditions—such as wind speed—and SST can cause LHF to vary. Thus LHF may be decomposed into atmospheric forcing and oceanic response. The latter arises from the SST dependence of evaporation and may be cast as a Newtonian cooling term by linearizing (1),

$$Q'_{EO} = \overline{Q_E}\left(\frac{1}{\bar{q}_s}\frac{d\bar{q}_s}{dT}\right)T', \qquad (2)$$

where the overbar and prime denote the mean and perturbation, respectively. The residual term $Q'_{EA} = Q'_E - Q'_{EO}$ is due mostly to atmospheric adjustments in wind speed, RH, and ΔT. The atmospheric forcing due to changes in wind speed, for example, may be obtained by linearizing (1) into $Q'_{EW} = \overline{Q_E}\,\frac{W'}{\overline{W}}$, commonly known as the wind-evaporation-SST (WES) feedback [*Xie and Philander*, 1994]. By the same argument, changes in solar radiation and sensible heat flux are also considered as atmospheric adjustments.

3.1. Inter-Model Variations

[7] Linear trends for the 100-year period are calculated using the least square method and averaged over the TIO (40°–120°E, 20°S–20°N). Changes in NHF for the 20th century are so small in models (Figure 2a) that its trend is hard to detect in a time series plot like Figure 1b. The following two subsections investigate how various flux components reach a balance that leads to the robust SST warming. Our convention for flux is downward positive.

[8] Net DLR increases in all models by 1.5–3.3 W/m^2. Increased GHG concentrations enhance DLR from the atmosphere, warming the ocean. The ocean warming increases water vapor in the atmosphere, leading to a further increase in DLR. This water vapor feedback [*Hall and Manabe*, 1999] at the surface is apparently stronger than the increased upward longwave radiation due to the SST warming; the scattering of net DLR displays a positive correlation with SST. Thus, net DLR in the Indian Ocean is a positive feedback amplifying the GHG-induced warming. Note that this surface feedback is different from that measured by changes in radiative flux at the top of the atmosphere [*Bony et al.*, 2006]. Inter-model correlation is suggestive but may not reflect accurately the physical relationship between variables examined.

[9] The Newtonian cooling (NtC) component of LHF is a linear function of and acts to dampen the SST warming, ranging from −2 to −10 W/m^2 among models (not shown). The atmospheric forcing (AtF) component of LHF is to warm the ocean, ranging from 3 to 7 W/m^2 (Figure 2d). The sensible heat flux trend is positive in all models (Figure 2e), clustered around 0.5 W/m^2, because of an air temperature trend slightly larger than that of SST. The origin of this differential warming between SST and air temperature needs further studies but radiative effects of increased GHG and water vapor probably contribute to the stronger warming in the atmosphere than ocean.

[10] A strong positive correlation between surface solar radiation and SST warming emerges among models (Figure 2b). At first glance, it may imply a positive feedback but increased SST usually causes convective cloud cover to increase over the warm TIO. Thus the inter-model correlation suggests that the spread in TIO warming is due chiefly to differences in the cloud response to GHG and aerosol forcing among models. Except CCCMA and CSIRO

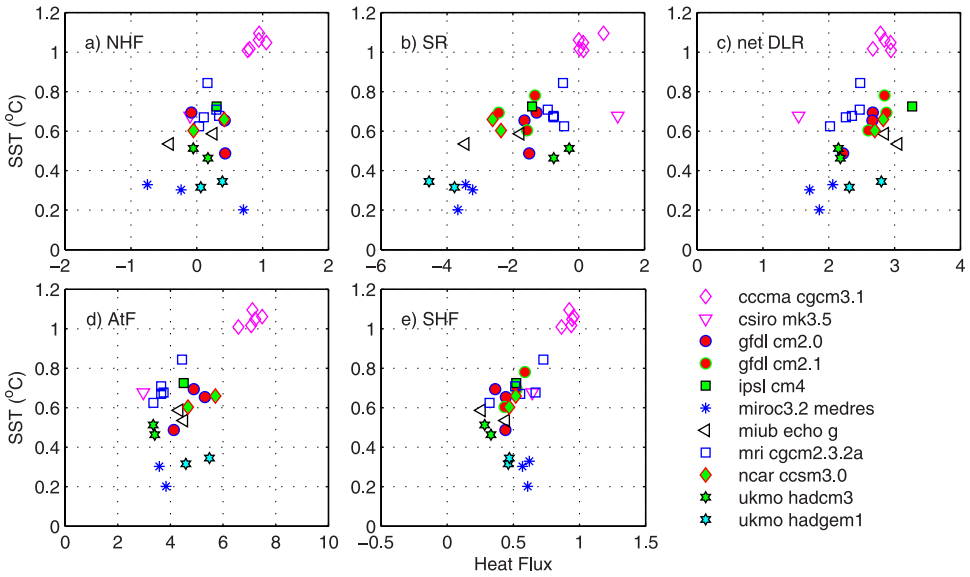

Figure 2. Scatter diagrams of changes in SST and surface heat flux components (W/m^2; downward positive): net surface heat flux (NHF), solar radiation (SR), net downward longwave radiation (net DLR), atmospheric forcing (AtF) component of the latent heat flux, and sensible heat flux (SHF). The change is defined as the linear trend for the 20th century. Different ensemble members for each model are presented with the same color and symbol.

models, the solar radiation trend is negative and acts to limit the TIO warming.

3.2. Ensemble Mean

[11] From an ocean mixed-layer point of view, the Newtonian cooling component of LHF represents the ocean response while all the other components are due to atmospheric forcing (including feedback). Figure 3 summarizes the forcing components and ocean response in multi-model ensemble mean. Net DLR is about 2.5 W/m^2, consisting of the GHG forcing and a feedback term due to changes in SST, water vapor and cloud. The latter is dominated by the water vapor feedback, estimated to be 1.6 W/m^2 using an observation-based empirical formula [*Gill*, 1982]

$$Q_L = 0.985\sigma T^4\left(0.39 - 0.05e_a^{1/2}\right)\left(1 - 0.6n_c^2\right) \qquad (3)$$

where σ is Stefan's constant, e_a surface water vapor pressure, n_c cloud cover. The difference from the net DLR change yields a GHG forcing of 0.9 W/m^2, similar in magnitude to direct radiative calculations [*IPCC*, 2007, Figure 2.23]. Solar radiation is a negative forcing at -1.6W/m^2.

[12] Atmospheric adjustments via LHF emerge as the dominant mechanism for the TIO warming: the atmospheric forcing component of LHF amounts to 4.5 W/m^2 while the sensible heat flux contributes another 0.5 W/m^2. At -5.7 W/m^2 (Figure 3), the Newtonian cooling of LHF nearly balances all the forcing terms. As a result, NHF is weakly positive at 0.2 W/m^2, in support of our initial hypothesis that the TIO warming is in quasi-equilibrium, with the atmospheric forcing and ocean response nearly in balance.

[13] We further decompose atmospheric forcing via LHF into components due to changes in wind speed, ΔT, and *RH*. Over TIO, the decreased wind contributes about 2.5 W/m^2. Atmospheric circulation in the tropics is predicted to slow down as tropospheric vapor increases at a faster rate than precipitation in response to global warming [*Held and Soden*, 2006]. Many studies assume that air-sea temperature difference and *RH* do not change in global warming, a good approximation for many purposes [*Held and Soden*, 2006]. At the surface indeed, *RH* increases only by 0.1%, and ΔT by 0.04°C over the TIO. These seemingly small changes contribute a total of 2 W/m^2 to the ocean warming, an amount comparable to the GHG forcing itself. Thus atmospheric feedback due to subtle changes in *RH* and

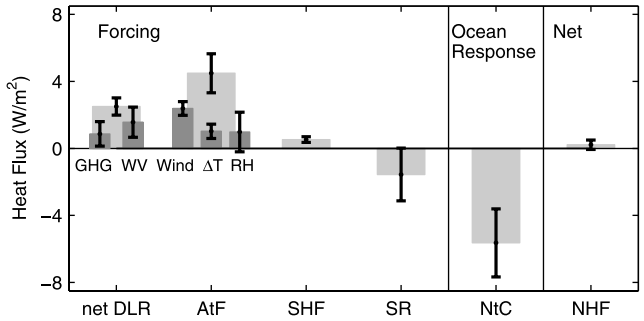

Figure 3. Linear trends in surface heat flux components. Each gray block presents the multi-model ensemble mean, along with the inter-model standard deviation in error bar. NtC stands for the Newtonian cooling component of the LHF, and other abbreviations are the same as in Figure 2. Net DLR includes the GHG forcing and water vapor (WV) feedback. The atmospheric forcing (AtF) component of the LHF is further decomposed into three terms due to the change in wind speed, air-sea temperature difference (ΔT), and relative humidity (*RH*).

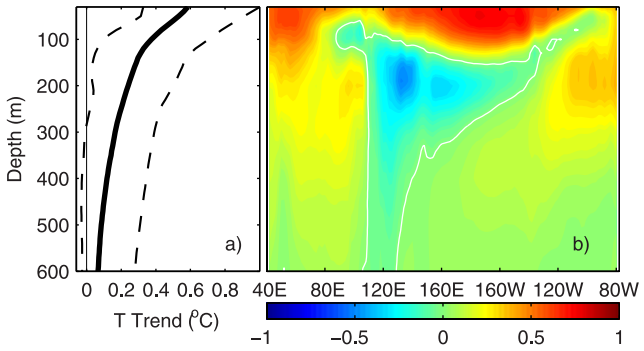

Figure 4. (a) Vertical structure of the 20th century temperature trend averaged over the TIO basin: 10-model ensemble mean (solid line), and the minimum and maximum among models (dashed lines). (b) Longitude-depth section of the temperature difference (°C; the zero contour in white) between last and first 20 years, averaged in (10°S–10°N) and with 7 models that show common subsurface cooling in the eastern Indian and western Pacific Oceans.

ΔT is not negligible in ocean heat budget, calling for further investigations into this overlooked feedback.

3.3. Vertical Structure

[14] The trend of TIO basin-mean temperature displays a surface-trapped structure in models (Figure 4a). The warming drops by half at 125 m. The observed temperature trend for 1960–1999 shows an even sharper surface trapping, confined above 125 m over TIO [*Pierce et al.*, 2006]. The surface trapped structure is consistent with small changes in NHF, which must be balanced by ocean advection and mixing. The surface trapped structure and small NHF changes suggest that the slab mixed layer is a good model for the basin-mean TIO warming during the 20th century but ocean circulation changes [*Lee*, 2004; *Pierce et al.*, 2006] may have significant effects on sub-basin scale SST anomalies.

[15] The reduced surface warming in the eastern equatorial Indian Ocean, accompanied by a subsurface cooling, deviates from the slab ocean model in the majority (7 out of 10) of the CMIP3 models explored (Figure 4b). Subsurface temperature anomalies in the equatorial Indo-Pacific Oceans are consistent with the slow down of the Walker Circulation anticipated in a warming climate. The subsurface zonal dipole is reminiscent of the Indian Ocean dipole [*Saji et al.*, 1999] and due to the relaxed westerly winds on the equator. A similar slow-down of the easterly winds in the equatorial Pacific relaxes the thermocline tilt there [*Han et al.*, 2006]. These subsurface anomaly patterns over the equatorial Indo-Pacific in 20th century runs are similar to those derived from A1B scenario runs under much large GHG forcing [*Vecchi and Soden*, 2007], albeit with reduced amplitudes.

4. Summary and Discussion

[16] We have investigated the mechanisms for the steady TIO warming in eleven CMIP3 models from a surface heat flux perspective. The results may be summarized in the following sequence of adjustments. Increased GHG concentrations increase downward longwave radiation and warm the TIO. The resultant tropospheric moistening amplifies the SST warming via longwave radiation. The warming also increases surface evaporation, a damping that balances atmospheric forcing/feedback. Besides the Newtonian cooling that arises from the SST dependency of evaporation, surface LHF contains an atmospheric forcing component; relaxed winds and slight increase in surface relative humidity and stability act to reduce evaporation, helping amplify the TIO warming. In most models, solar radiation is a negative forcing that reduces the TIO warming. It displays a large inter-model variability, causing much of the spread in the magnitude of the SST warming among models.

[17] The NHF change is much smaller than the components discussed above, suggesting a first-order balance among GHG forcing, atmospheric adjustments, and the ocean Newtonian damping. Twice of net DLR, the atmospheric adjustment via surface turbulent heat flux is the dominant warming mechanism (Figure 3). Without this feedback, the warming under surface flux equilibrium would be substantially reduced; a much weaker Newtonian cooling of -0.9 W/m^2, instead of -5.7 W/m^2 in CMIP3 simulations, would be sufficient to balance radiation fluxes.

[18] The LHF increase in the warming climate is much smaller than that expected from the Clausius-Clapeyron equation, with LHF/NtC = 0.23. As surface evaporation balances precipitation on global average, the small LHF increase is consistent with a slower rate of increase in precipitation than specific humidity, a robust result among models that implies a slow down of tropical circulation [*Held and Soden*, 2006]. Our results show that relaxed wind, increased stability and *RH* slow the rate of LHF increase (Figure 3). The decomposition of global surface evaporation supports this conclusion (I. Richter, personal communication, 2007).

[19] The net flux change for the 20th century is only 0.2 W/m^2 in models, far below the detection limit of observations [*Yu et al.*, 2007]. Consistent with the quasi-equilibrium heat flux adjustments, the warming is trapped in the top 125 m in the TIO. To the extent that mixing with the pre-warming subsurface ocean weakens the surface warming, the weak coupling between the surface and subsurface ocean may explain why the observed SST warming since 1950s is most pronounced over the TIO (Figure 1a).

[20] **Acknowledgments.** We wish to thank J. Hafner and APDRC for maintaining the local database. This work is supported by the U.S. National Science Foundation, the Japan Agency for Marine-Earth Science and Technology, and the Chinese Academy of Sciences. IPRC/SOEST publication 517/7403.

References

Alory, G., S. Wijffels, and G. Meyers (2007), Observed temperature trends in the Indian Ocean over 1960–1999 and associated mechanisms, *Geophys. Res. Lett.*, *34*, L02606, doi:10.1029/2006GL028044.

Bony, S., et al. (2006), How well do we understand and evaluate climate change feedback processes?, *J. Clim.*, *19*, 3445–3482.

Giannini, A., R. Saravanan, and P. Chang (2003), Oceanic forcing of Sahel rainfall on interannual to interdecadal time scales, *Science*, *302*, 1027–1030.

Gill, A. E. (1982), *Atmosphere-Ocean Dynamics*, 662 pp., Academic, New York.

Hall, A., and S. Manabe (1999), The role of water vapor feedback in unperturbed climate variability and global warming, *J. Clim.*, *12*, 2327–2346.

Han, W., G. A. Meehl, and A. Hu (2006), Interpretation of tropical thermocline cooling in the Indian and Pacific oceans during recent decades, *Geophys. Res. Lett.*, *33*, L23615, doi:10.1029/2006GL027982.

Held, I. M., and B. J. Soden (2006), Robust response of the hydrological cycle to global warming, *J. Clim.*, *19*, 5686–5699.

Hoerling, M. P., J. W. Hurrell, T. Xu, G. T. Bates, and A. S. Phillips (2004), Twentieth century North Atlantic climate change. part II: Understanding the effect of Indian Ocean warming, *Clim. Dyn.*, *23*, 391–405.

Intergovernmental Panel on Climate Change (IPCC) (2007), *Climate Change 2007: The Physical Science Basis*, edited by S. Solomon et al., 996 pp., Cambridge Univ. Press, Cambridge, UK.

Knutson, T. R., et al. (2006), Assessment of twentieth-century regional surface temperature trends using the GFDL CM2 coupled models, *J. Clim.*, *19*, 1624–1651.

Lau, N.-C., A. Leetmaa, and M. J. Nath (2006), Attribution of atmospheric variations in the 1997–2003 period to SST anomalies in the Pacific and Indian ocean basins, *J. Clim.*, *19*, 3607–3627.

Lee, T. (2004), Decadal weakening of the shallow overturning circulation in the South Indian Ocean, *Geophys. Res. Lett.*, *31*, L18305, doi:10.1029/2004GL020884.

Pierce, D. W., T. P. Barnett, K. M. AchutaRao, P. J. Glecker, J. M. Gregory, and W. M. Washington (2006), Anthropogenic warming of the oceans: Observations and model results, *J. Clim.*, *19*, 1873–1900.

Saji, N. H., B. N. Goswami, P. N. Vinayachandran, and T. Yamagata (1999), A dipole mode in the tropical Indian Ocean, *Nature*, *401*, 360–363.

Smith, T. M., and R. W. Reynolds (2004), Improved extended reconstruction of SST (1854–1997), *J. Clim.*, *17*, 2466–2477.

Vecchi, G. A., and B. J. Soden (2007), Global warming and the weakening of the tropical circulation, *J. Clim.*, *20*, 4316–4340.

Xie, S.-P., and S. G. H. Philander (1994), A coupled ocean-atmosphere model of relevance to the ITCZ in the eastern Pacific, *Tellus, Ser. A*, *46*, 340–350.

Yang, J., Q. Liu, S.-P. Xie, Z. Liu, and L. Wu (2007), Impact of the Indian Ocean SST basin mode on the Asian summer monsoon, *Geophys. Res. Lett.*, *34*, L02708, doi:10.1029/2006GL028571.

Yu, L., X. Jin, and R. A. Weller (2007), Annual, seasonal, and interannual variability of air-sea heat fluxes in the Indian Ocean, *J. Clim.*, *20*, 3190–3209.

Y. Du and S.-P. Xie, International Pacific Research Center, SOEST, University of Hawaii at Manoa, Honolulu, HI 96822, USA. (yandu@hawaii.edu; xie@hawaii.edu)